Monthly Notices
of the
ROYAL ASTRONOMICAL SOCIETY

MNRAS **451,** 3287–3298 (2015) doi:10.1093/mnras/stv1124

A new method based on the subpixel Gaussian model for accurate estimation of asteroid coordinates

V. E. Savanevych,[1⋆] O. B. Briukhovetskyi,[2] N. S. Sokovikova,[1⋆] M. M. Bezkrovny,[3] I. B. Vavilova,[4⋆] Yu. M. Ivashchenko,[4,5] L. V. Elenin,[6] S. V. Khlamov,[1] Ia. S. Movsesian,[1] A. M. Dashkova[3] and A. V. Pogorelov[1]

[1]*Kharkiv National University of Radio Electronics, 14 Lenin Ave, Kharkiv UA-61166, Ukraine*
[2]*Kharkiv Representation of the General Customer's Office of the State Space Agency of Ukraine, 1 Akademika Proskury St, Kharkiv UA-61070, Ukraine*
[3]*Zaporizhya Institute of Economics and Information Technologies, 16-B Kiyashka St, Zaporizhya UA-69015, Ukraine*
[4]*Main Astronomical Observatory of the NAS of Ukraine, 27 Akademika Zabolotnogo St, Kyiv UA-03680, Ukraine*
[5]*Andrushivka Astronomical Observatory, Galchyn, Zhytomyr Region UA-13400, Ukraine*
[6]*Keldysh Institute of Applied Mathematics of the RAS, 4 Miusskaya Sq., Moscow 125047, Russia*

Accepted 2015 May 15. Received 2015 May 13; in original form 2014 August 7

ABSTRACT

We describe a new iteration method to estimate asteroid coordinates, based on a subpixel Gaussian model of the discrete object image. The method operates by continuous parameters (asteroid coordinates) in a discrete observational space (the set of pixel potentials) of the CCD frame. In this model, the kind of coordinate distribution of the photons hitting a pixel of the CCD frame is known a priori, while the associated parameters are determined from a real digital object image. The method that is developed, which is flexible in adapting to any form of object image, has a high measurement accuracy along with a low calculating complexity, due to the maximum-likelihood procedure that is implemented to obtain the best fit instead of a least-squares method and Levenberg–Marquardt algorithm for minimization of the quadratic form. Since 2010, the method has been tested as the basis of our Collection Light Technology (CoLiTec) software, which has been installed at several observatories across the world with the aim of the automatic discovery of asteroids and comets in sets of CCD frames. As a result, four comets (C/2010 X1 (Elenin), P/2011 NO1(Elenin), C/2012 S1 (ISON) and P/2013 V3 (Nevski)) as well as more than 1500 small Solar system bodies (including five near-Earth objects (NEOs), 21 Trojan asteroids of Jupiter and one Centaur object) have been discovered. We discuss these results, which allowed us to compare the accuracy parameters of the new method and confirm its efficiency. In 2014, the CoLiTec software was recommended to all members of the *Gaia*-FUN-SSO network for analysing observations as a tool to detect faint moving objects in frames.

Key words: methods: data analysis – techniques: image processing – comets: general – minor planets, asteroids: general.

1 INTRODUCTION

There are many methods for determining an asteroid's position during observations with a CCD camera. For example, the full width at half magnitude (FWHM) approach (Gary & Healy 2006), which is based on the analytical description of the object images on the CCD frame, as well as other methods in which the position of an object's maximum brightness on a CCD image is taken as its coordinates (Miura, Itagaki & Baba (2005)).

Most of these methods have a common feature. They use point-spread function (PSF) fitting to approximate the object image and obtain information about regularities in the distribution of the registered photons on the CCD frame (for details, see Gural, Larsen & Gleason 2005; Yanagisawa et al. 2005; Lafreniere & Marois 2007; Zacharias 2010; Dell'Oro & Cellino 2012; Veres & Jedicke 2012). Among the models of photon distribution that are used more often, we note the two-dimensional Gaussian model (Jogesh Babu et al. 2008; Zacharias 2010; Veres & Jedicke 2012), Moffat model (Bauer 2009; Izmailov et al. 2010) and Lorentz model (Izmailov et al. 2010; Zacharias 2010). These models are usually described by continuous functions, while the CCD images are discrete. Such an approach was criticized, reasonably, by Bauer (2009). The principal disadvantage is that these models work well only with a large amount of data. This leads to the fact that first the computation process becomes much more complicated and secondly the problem relating to the

⋆ E-mail: vadym@savanevych.com (VES); nataly.sokovikova.gmail.com (NSS); irivav@mao.kiev.ua (IBV)

© 2015 The Authors
Published by Oxford University Press on behalf of the Royal Astronomical Society

adequacy of estimations of PSF parameters used cannot be solved. As a result, the error in the coordinate determination of observed celestial objects must be increasing.

In addition to the aforementioned disadvantage, existing methods do not pay sufficient attention to taking the noise component of the object image into account. It is assumed that its registration and compensation are performed during the preliminary stage of image processing (Gural et al. 2005) or that the object image is exempt from noise according to the accepted signal-to-noise (SNR) model (Lafreniere & Marois 2007; Izmailov et al. 2010). At the same time, the error introduced by the operation of removing the noise component from the object image is not considered in the subsequent procedure of coordinate determination.

The errors in CCD astrometry are traditionally divided into instrument, reduction, reference catalogue and measurement errors. The first type traditionally includes errors in instrumental parameters such as shutter delay and clock correction, which result in incorrect timing. The second error category (reduction) is associated with the method relating to standard and measured coordinates and depends on the choice of algorithm relation between these coordinates. For example, being not significant for the wide-angle astrographs, such an error depends strongly on the choice of type and degree of polynomial approximation in the Turner method. It is important to note that a systematic error in timing is not shared with the coordinate error while tracking an object in the sky, so it must be caught clearly with a reliable shutter sync.

The reference catalogue errors are divided into three main classes: zonal errors (systematic errors of the reference catalogue), coordinate errors of reference stars in the catalogue epoch and proper-motion errors of reference stars. Therefore, the choice of reference catalogue is very important. For example, *Hipparcos* or Tycho catalogues had no errors at the epoch 1990.0, because the intrinsic accuracy was at the level of milliseconds of arc, but for the present epoch there is a necessity to take into account the proper-motion errors of reference stars. The solution of this problem, i.e. the creation of a huge new data base of proper motions of stars, is one of the tasks of the *Gaia* mission. It is worth noting that the choice of reference catalogue is not so important when monitoring observations of the sky are conducted with the aim of discovering new Solar system small bodies, because the intrinsic accuracy of a catalogue should not necessarily be maximized compared with those for the following tracking of the object discovered.

The measurement error is related, first of all, to the determination of the coordinates of the image centre or the accuracy of a digital approximation of the CCD image (fitting). An attempt to improve the fitting may not lead to the expected results if the reference catalogue errors and timing are not taken attentively into account.

Each of the aforementioned factors could be the source of both systematic and random errors. Any attempt to reduce one of these errors is impossible without control of other factors. Therefore, the task of the observers is to be responsible for monitoring all possible sources of errors. The aim of this article is to help observers to refine the coordinate measurements of the object image on the CCD frame and to control the errors in the measured coordinates.

With this aim, we developed a new method for estimating asteroid coordinates accurately on a set of CCD frames, based on a subpixel Gaussian model of the discrete image of an object. In this model, the form of the coordinate distribution of photons hitting a pixel on the CCD frame is known a priori, while its parameters can be determined from the real digital image of the object. Our method has low computational complexity due to the use of equations of maximum likelihood; additionally, the proposed model is more flexible, adapting to any form of real image of the object. For example, in fact the PSF is a superpixel function, because it describes the changes in the brightness of pixels of a celestial object image. We propose to use the density function of the coordinates of arriving photons from a celestial object instead of the PSF. This function is a subpixel one. To obtain the PSF from this function, it should be integrated over the area of determination of each image pixel of an object or compact group of objects. It turns out that subpixel models are more flexible and may describe the real image more adequately. This effect does not occur in the case of bright objects. However, applying a more flexible model for faint objects, we are able to improve the accuracy of the measurements (compared with Astrometrica, for example) by 30–50 per cent (more details are given in the discussion). Our method also takes into account the principal peculiarities of object image formation on the CCD frame, along with the possible irregular distribution of the residual noise component, both on the object image and in its vicinity.

Some generalizations of the proposed method are presented in our previous works (Savanevych 1999, 2006; Savanevych et al. 2010, 2011, 2012, 2014; Vavilova et al. 2011, 2012a,b). Since 2010, due to its application through the CoLiTec software, which was installed at several observatories around the world, four comets (C/2010 X1 (Elenin), P/2011 NO1(Elenin), C/2012 S1 (ISON) and P/2013 V3 (Nevski)) and more than 1500 small Solar system bodies (including five near-Earth Objects (NEOs), 21 Trojan asteroids of Jupiter and one Centaur object) have been discovered. These results confirm the efficiency of the proposed method. The main stages of image processing with the CoLiTec software are presented in Fig. 1.

The structure of this article is as follows: we describe a problem statement and the method in Sections 2 and 3, respectively. Results based on the testing of this method with the CoLiTec software are presented in Section 4. We compare and discuss the accuracy and other parameters for determining the position of the faint celestial object on the CCD frame obtained by the proposed method and others in Section 5. Concluding remarks are given in Section 6.

2 PROBLEM STATEMENT

If the exposure time is small, the shift of asteroid position in the sky can be ignored. In this case, asteroid and field stars are imaged as blur spots rather than points on the CCD frame. It is postulated that the coordinates of the signal photons from asteroids and stars hitting the CCD frame have a circular normal distribution, with mathematical expectations x_t, y_t and mean-square error (MSE) σ_{ph}.

It is supposed that a preliminary detection of the asteroid has already been conducted before the determination of its coordinates. The result of this detection is a preliminary estimation of the asteroid position on the CCD frame, namely the determination of the coordinates of the pixel that corresponds to the maximum brightness peak on the asteroid image. We name the set of pixels around this pixel as the area of intraframe processing (AIFP). Thus, the AIFP size (N_{IPS}, in pixels) is much larger than the image of the asteroid.

The original CCD image of the celestial object contains harmful interference such as read noise, dark currents, irregularity in the pixel-to-pixel sensitivity, sky-background radiation, etc. (Harris 1990; Faraji & MacLean 2006). Hence the CCD frame can be represented as an additive mix of the images of celestial objects and a component formed by this generalized interference. Within the scope of the whole CCD frame, the interference component has a complex structure. However, in the near vicinity of the asteroid image under study, such an interference component can be described

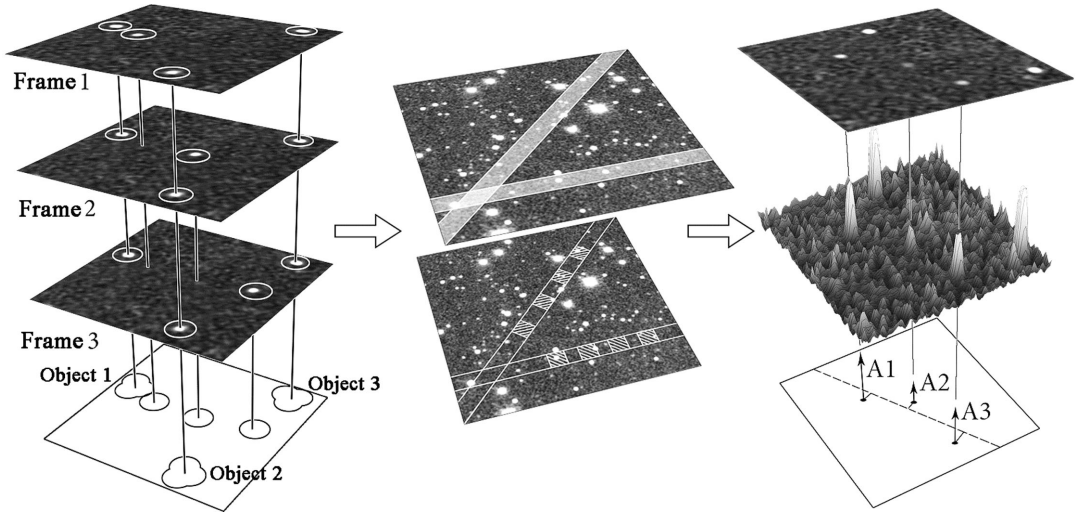

Figure 1. The main steps of object image processing in the CoLiTec software: (a) exclusion of stationary objects; (b) detection of moving objects; (c) analysis of moving objects, where A1, A2, and A3 outline coordinate deviations of moving objects from their trajectory.

with good accuracy as a plane with arbitrary slope. Such a representation describes the interference component well, especially if there is a bright object in the vicinity of the AIFP being studied.

The output signals of the CCD matrix pixels $N_{\rm IPS}$ are easily reduced to the relative frequencies ν^*_{ikt} of the photons hitting the $ik^{\rm th}$ pixel on the $t^{\rm th}$ frame:

$$\nu^*_{ikt} = \frac{A_{ikt}}{\sum\limits_{i,k}^{N_{\rm IPS}} A_{ikt}}, \tag{1}$$

where A_{ikt} is the brightness of the ikth pixel of the CCD matrix.

The result of the observation is then the set $\tilde{U} = \nu^*_{11t}, ..., \nu^*_{ikt}, ..., \nu^*_{N_{\rm IPSt}}$ of relative frequencies, which are independent of each other. The theoretical analogues of the measured relative frequencies are the probabilities $\nu_{ikt}(\Theta)$ that during the exposure time the photons hit the $ik^{\rm th}$ pixel of the CCD matrix with borders $x_{{\rm beg}i}$, $x_{{\rm end}i}$ in coordinate x and $y_{{\rm beg}k}$, $y_{{\rm end}k}$ in coordinate y on the $t^{\rm th}$ frame. It is supposed that the angular sizes of the pixel, Δx and Δy, are the same in both coordinates x and y.

Thus, the problem statement is as follows: we need to develop a method of maximum-likelihood estimation of asteroid coordinates on the $t^{\rm th}$ CCD frame using the set of relative frequencies ν^*_{ikt}. It is believed that the likelihood function is differentiable in the vicinity of its global maximum and its initial approximation is also in the same vicinity. The set of estimated parameters Θ includes the asteroid coordinates x_t and y_t on the $t^{\rm th}$ frame and the mean-square error of the coordinates of photons hitting the CCD matrix, $\sigma_{\rm ph}$.

To introduce the new method, we use two functions. The density distribution of a normally distributed random variable z with mathematical expectation m_z and dispersion σ^2 is determined by the expression

$$N_z(m_z, \sigma^2) = \frac{1}{\sqrt{2\pi\sigma}} \exp\left[-\frac{1}{2\sigma^2}(z - m_z)^2\right]. \tag{2}$$

The probability F_z that a random variable z is within the closed interval $[z_{\rm beg}, z_{\rm end}]$ is

$$F_{zi}(m_z, \sigma^2) = \int_{z_{\rm end}}^{z_{\rm beg}} N_z(m_z; \sigma^2)\,{\rm d}z. \tag{3}$$

3 TASK SOLUTION

To achieve the maximum accuracy of estimation of an object position on the frame, the discretization factor needs to be taken into account, because we estimate continuous parameters (coordinates of objects) at a discrete set of measured values (the brightness of the CCD matrix pixels). The general view of maximum-likelihood estimation of the object position can be expressed by

$$\sum_{i,k}^{N_{\rm IPS}} \frac{\nu^*_{ikt}}{\nu_{ikt}(\Theta)} \frac{\partial \nu_{ikt}(\Theta)}{\partial \Theta_m} = 0, \tag{4}$$

where Θ is the set of the estimated parameters x_t, y_t and $\sigma_{\rm ph}$.

The relation between the probability $\nu_{ikt}(\Theta)$ that photons hit the $ik^{\rm th}$ pixel (equation 4) and the function of coordinate distribution $f(x, y)$ of the incidence of photons from the object on the CCD matrix has the form

$$\nu_{ikt}(\Theta) = \int_{x_{{\rm beg}i}}^{x_{{\rm end}i}} \int_{y_{{\rm beg}k}}^{y_{{\rm end}k}} f(x, y)\,{\rm d}x\,{\rm d}y. \tag{5}$$

After compensation for the noise component on the CCD image, the function $f(x, y)$ could be expressed as a weighted mix of normal and uniform probability distributions:

$$f(x, y, \Theta) = p_0 + \frac{p_1}{2\pi\sigma^2_{\rm ph}} \exp\left\{-\frac{1}{2\sigma^2_{\rm ph}}[(x - x_t)^2 + (y - y_t)^2]\right\}, \tag{6}$$

where $p_1 = 1 - p_0$ is the relative weight of the signal photons of the object; p_0 $(0 \le p_0 < 1)$ is the relative weight of the residual noise photons of the CCD matrix after compensation for flat generalized interference; x_t and y_t are the object coordinates on the $t^{\rm th}$ frame at time t^t, corresponding to the mathematical expectations of the coordinates of incidence of the signal photons.

The probability (equation 5) that photons hit the CCD matrix pixels can be written as follows:

$$\nu_{ikt}(\Theta) = I_{ikt{\rm noise}} + I_{ikts}, \tag{7}$$

where $I_{ikts} = p_i F_{xi}(xi; \sigma^2_{\rm phi}) F_{\rm yk}(y_t, \sigma^2_{\rm ph})$ is the probability that signal photons I_{ikt} hit the $ik^{\rm th}$ pixel of the CCD matrix and $I_{ikt{\rm noise}} = \Delta^2_{{\rm CCD}p0}$ is the probability that the noise residual photons hit the $ik^{\rm th}$ pixel of the CCD matrix, where $\Delta_{\rm CCD} = \Delta_x = \Delta_y$.

The derivative of the probability (equation 7) in the x coordinate is determined by the expression

$$\frac{\mathrm{d}\nu_{ikt}(\Theta)}{\mathrm{d}x_t} = \frac{p_1 F_{\mathrm{yk}}(y_t;\sigma^2_{\mathrm{ph}})F_{xi}(x_t;\sigma^2_{\mathrm{ph}})}{\sigma_{\mathrm{ph}}}(m^{\mathrm{loc}}_{xi} - x_t), \tag{8}$$

where

$$m^{\mathrm{loc}}_{xi} = m_x + \frac{\sigma^2}{F_{xi}(m_x;\sigma^2)}\left[N_{\mathrm{xendi}}(m_x;\sigma^2) - N_{\mathrm{xbegi}}(m_x;\sigma^2)\right]$$

is the local (on the closed interval $[x_{\mathrm{begi}}; x_{\mathrm{endi}}]$) mathematical expectation of a normally distributed random value x with mathematical expectation m_x and dispersion σ^2. The derivative of the probability (equation 7) in the y coordinate has the same expression as equation (8).

The system of equations of maximum likelihood for the AIFP pixels studied in the case in which the asteroid position is only estimated will take the form

$$\begin{cases} \hat{x}_t = \dfrac{\sum_{i,k}^{N_{\mathrm{IPS_s}}} \nu^*_{ikt}\lambda_{ikt}m^{\mathrm{loc}}_{xi}}{\sum_{i,k}^{N_{\mathrm{IPS_s}}} \nu^*_{ikt}\lambda_{ikt}}, \\ \hat{y}_t = \dfrac{\sum_{i,k}^{N_{\mathrm{IPS_s}}} \nu^*_{ikt}\lambda_{ikt}m^{\mathrm{loc}}_{\mathrm{yk}}}{\sum_{i,k}^{N_{\mathrm{IPS_s}}} \nu^*_{ikt}\lambda_{ikt}}, \end{cases} \tag{9}$$

where $N_{\mathrm{IPS_s}}$ is the quantity of pixels in part of the AIFP area (the area where the signal from the object is expected), $\hat{x}_t$ and $\hat{y}_t$ are estimations of the asteroid coordinates and λ_{ikt} is the fraction of photons from the celestial object in the ik^{th} pixel of the t^{th} CCD frame. The latter value is determined by

$$\lambda_{ikt} = \frac{p_1 F_{\mathrm{yk}}(y_t;\sigma^2_{\mathrm{ph}})F_{xi}((x_t;\sigma^2_{\mathrm{ph}})}{\nu_{ikt}(\Theta)}. \tag{10}$$

To estimate the MSE of the coordinates of photons hitting the CCD frame from the asteroid, we use the equation of maximal likelihood:

$$\hat{\sigma}^2_{\mathrm{ph}} = \frac{\sum_{i,k}^{N_{\mathrm{IPS_s}}} \nu^*_{ikt}\lambda_{ikt}\left[\left(m^{\mathrm{loc}}_{xi} - \hat{x}_t\right)^2 + \left(m^{\mathrm{loc}}_{\mathrm{yk}} - \hat{y}_t\right)^2\right]}{2\sum_{i,k}^{N_{\mathrm{IPS_s}}} \nu^*_{ikt}\lambda_{ikt}}. \tag{11}$$

We cannot exclude generalized noise interference completely. For this reason, to take into account the relative weight of the signal photons, we use a standard estimation of the weights of the discrete mix of probability distributions (Lo, Mendell & Rubin 2001):

$$\hat{p}_1 = \frac{1}{N_{\mathrm{IPS_s}}}\sum_{i,k}^{N_{\mathrm{IPS_s}}}\lambda_{ikt}; \qquad \hat{p}_0 = 1 - \hat{p}_1. \tag{12}$$

Therefore, the local mathematical expectation of the coordinates of object position is a function of the relevant coordinates and equation (9) gives a system of transcendental equations that can be solved by the method of successive approximations (see e.g. Burden & Faires 2010).

The algorithm for the estimation of object coordinates consists of two successive operations. The first operation is to split the statistics of the AIFP pixels into the statistics of the signal and the statistics of the residual interference. This is done for pixels from the AIFP area where the object is expected. According to the Θ values calculated from the previous iteration, the photons of the pixel are divided into those belonging to the object and those belonging to the residual interference. The photons belonging to the object are analysed to determine the estimation of its position. Thus, the coordinates of the local maximum in the object image around which the AIFP area is formed are used as the initial approximation. The result of this operation is a set of split coefficients λ_{ikt}.

The second operation provides an estimation of the object coordinates based on the statistics obtained during the operation of splitting. It is conducted in a strongly determined way from equations (9)– (12). The result $\hat{\Theta}_n$ of this operation serves as an initial approximation for the operation of splitting at the next iteration step. The iteration process is continued until the difference between $\hat{\Theta}_n$ and $\hat{\Theta}_{n-1}$ becomes smaller than the predetermined value, for example 0.1 per cent of the angle size of a pixel.

Analysis of the iteration process shows that convergence is provided while the following conditions are fulfilled:

$$\mathrm{d}x = \frac{|x_0 - x_{\mathrm{true}}|}{\sigma_x} < 6, \qquad \mathrm{d}y = \frac{|y_0 - y_{\mathrm{true}}|}{\sigma_y} < 6, \tag{13}$$

where $\mathrm{d}x$ and $\mathrm{d}y$ are the relative distances between the initial and actual positions of the object, x_0 and y_0 are the initial approximations of the object coordinates, x_{true} and y_{true} are the actual object coordinates and σ_x and σ_y are the MSEs of the coordinates of signal photons hitting the CCD matrix.

Observations based on the proposed method have shown that this condition is almost always fulfilled for real images of asteroids and stars and, in most cases, the relative distance is not more than ∼1.0–15.

The opportunity to divide the AIFP area into an interference area (pixels that have registered photons only from interference) and an object area (pixels that have registered photons from both object and interference) yields a more simple and reliable algorithm for estimation of the flat interference component (compared with estimation in the common system of maximum-likelihood equations). Namely, there is an independent estimation by the method of least squares (MLS). Thus, the density of the coordinate distribution of photons from the residual interference will represent an equation for a plane with an arbitrary slope:

$$f_{\mathrm{noise}}(x, y) = A_{\mathrm{noise}}x + B_{\mathrm{noise}}y + C_{\mathrm{noise}}. \tag{14}$$

The probability that these photons will hit the ik^{th} pixel can be given by analogy with equation (5):

$$\nu^*_{ikt\mathrm{noise}}(\Theta_{\mathrm{noise}}) = A^{\mathrm{int}}_{\mathrm{noise}}x_{ik} + B^{\mathrm{int}}_{\mathrm{noise}}y_{ik} + C^{\mathrm{int}}_{\mathrm{noise}}, \tag{15}$$

where $\nu^*_{ikt\mathrm{noise}}$ is the measured frequency of the noise photons hitting the ik^{th} pixel of the CCD matrix; $A^{\mathrm{int}}_{\mathrm{noise}} = \Delta^2_{\mathrm{CCD}}A_{\mathrm{noise}}$, $B^{\mathrm{int}}_{\mathrm{noise}} = \Delta^2_{\mathrm{CCD}}B_{\mathrm{noise}}$, $C^{\mathrm{int}}_{\mathrm{noise}} = \Delta^2_{\mathrm{CCD}}C_{\mathrm{noise}}$, $\Theta^{\mathrm{T}}_{\mathrm{noise}} = (A^{\mathrm{int}}_{\mathrm{noise}}, B^{\mathrm{int}}_{\mathrm{noise}}, C^{\mathrm{int}}_{\mathrm{noise}})$ are the integral parameters of the flat noise component and its vectors; $x_{ikt} = (x_{\mathrm{endi}} + x_{\mathrm{begi}})/2$, $y_{ikt} = (y_{\mathrm{endk}} + y_{\mathrm{begk}})/2$ are the average values of coordinates of the ik^{th} pixel.

Thus, the probabilities that noise photons will hit the pixels of the AIFP studied depend linearly on the angle coordinates of the centres x_j and y_j of these pixels and represent, in themselves, a plane with integral parameters $A^{\mathrm{int}}_{\mathrm{noise}}$, $B^{\mathrm{int}}_{\mathrm{noise}}$ and $C^{\mathrm{int}}_{\mathrm{noise}}$. It is worth noting that the pixels containing the supposed object image should be eliminated before determination of the noise parameters.

The integral parameters of the flat interference component, $A^{\mathrm{int}}_{\mathrm{noise}}$, $B^{\mathrm{int}}_{\mathrm{noise}}$ and $C^{\mathrm{int}}_{\mathrm{noise}}$, can be determined with a linear MLS estimation:

$$\hat{\Theta}_{\mathrm{noise}} = (F^{\mathrm{T}}F)^{-1}F^{\mathrm{T}}\tilde{U}_{\mathrm{noise}}, \tag{16}$$

where

$$F^{\mathrm{T}} = \begin{Vmatrix} x_1 & \ldots & xi & \ldots & x_{N_{\mathrm{IPSnoise}}} \\ y_1 & \ldots & y_i & \ldots & y_{N_{\mathrm{IPSnoise}}} \\ 1 & \ldots & 1 & \ldots & 1 \end{Vmatrix}, \tag{17}$$

where x_j and y_j are the angular coordinates of the j^{th} pixel, which is used to estimate the parameters of the flat interference component,

and $N_{\mathrm{IPS_{noise}}}$ is the number of AIFP pixels that do not contain the object image.

To obtain the integral parameters (equations 16 and 17), only those AIFP pixels not belonging to areas with object images ($N_{\mathrm{IPSnoise}} \leq (N_{\mathrm{IPS}} - N_{\mathrm{IPSs}})$) should be used. To exclude the influence of anomalous emissions of brightness in the pixels, we apply two iterations of MLS. In the second iteration, we use only those pixels for which the value of the frequency obtained, $\nu^*_{iktnoise}$, satisfies the following condition:

$$|\nu^*_{iktnoise} - \hat{\nu}^*_{iktnoise}| \leqslant k_{noise} \sqrt{\frac{\sum_{i,k}^{N_{\mathrm{IPSnoise}}} (\nu^*_{iktnoise} - \hat{\nu}^*_{iktnoise})^2}{N_{\mathrm{IPS_{noise}}}}}, \tag{18}$$

where k_{noise} is the threshold coefficient for removing those pixels that do not satisfy this condition, for example $k_{noise} = 3$,

$$\sqrt{\frac{\left(\sum_{i,k}^{N_{\mathrm{IPSnoise}}}\right)\left(\nu^*_{iktnoise} - \hat{\nu}^*_{iktnoise}\right)^2}{N_{\mathrm{IPSnoise}}}}$$

are the standard deviations of the flat interference component and $\hat{\nu}^*_{iktnoise} = \hat{A}^{int}_{noise} x_{i_t} + \hat{B}^{int}_{noise} y_{k_t} \hat{C}^{int}_{noise}$ is the smoothed estimation of the measured frequency of the ik^{th} pixel that is a part of the N_{IPSnoise} value given in equation (16).

The number of pixels N_{IPSnoise} determining the set $\tilde{U}_{noise}$ is reduced by such an amount for which the condition (equation 18) is not satisfied. The process is repeated until one of the following conditions is satisfied: (1) the module of difference of the two related values of standard deviation becomes less than a certain value; (2) the number of pixels N_{IPSnoise} becomes less than a given number; (3) the number of iterations exceeds a predetermined limit.

The next step is as follows: the values of the integral parameters of the flat interference component obtained are subtracted from the object signal of the given AIFP:

$$\nu^*_{iktS} = \nu^*_{iktS} - \left(\hat{A}^{int}_{noise} x_{it_s} + \hat{B}^{int}_{noise} y_{kt_s} + \hat{C}^{int}_{noise}\right), \tag{19}$$

where ν^*_{iktS} is the measured frequency of the photons hitting the ik^{th} pixel from the AIFP area and x_{its} and y_{kts} are the angular coordinates of the ik^{th} pixel from the AIFP area.

The AIFP area for the calculation of the flat interference component of the object image is set by the operator (the default is 31 × 31 pixels). If the size of the object image is larger, then the size of the area for the flat interference component is taken as the size of the object image multiplied by two (this is also set by the operator). As regards the area of frame for fitting, we note that fitting is carried out on the pixels that belong to the object image. Determination of these pixels is conducted through the delineation procedure, i.e. fitting is carried out not for a fixed area but for an area that depends on the size of the object image.

The principal stages of object image processing in the CoLiTec software are demonstrated by the pipeline shown in Fig. 1. They include (a) exclusion of stationary objects, (b) detection of moving objects and (c) analysis of moving objects, where A1, A2 and A3 outline the coordinate deviations of moving objects from their trajectory. If necessary, the measurements can be stacked, but only unstacked frames are processed statistically. Image service files (flat – bias – dark) can be used during the calibration process, but we offer an alignment frame option, which is commonly used. For example, to align frames we used a high-pass Fourier filter in the earlier versions of the CoLiTec software. Currently we are using median filtering, which has almost the same quality but is substantially faster. To select moving objects, measurements (blobs) are formed in all selected object images. After this, frames should be identified with each other and the coordinates of all measurements should be converted to the coordinate system of the basic frame.

The algorithm for the proposed method, which could be helpful in implementation, works as follows.

(1) To form a square area of intraframe processing (AIFP) for study with a side length of l pixels ($N_{\mathrm{IPS_s}}=s^2$) and a square region of presupposed existence of images of celestial objects with a side of s pixels ($s \ll l$). The centres of these regions are the local maxima of the image of an object (asteroid, comet, etc.) discovered previously.

(2) To conduct a multipass MLS estimation of parameters of the interface noise component according to equations (15) and (17). In this, only those pixels for which the value of the relative frequency ν^*_{ikt} (equation 1) satisfies the condition given by equation (18) are processed at the next MLS estimation pass. This 'do–while' loop is repeated as long as necessary for the module of difference of the two standard deviation values obtained sequentially to become smaller than a predetermined value.

(3) To exclude noise photons from the potentials of pixels in a region of presupposed existence of images of celestial objects according to equation (19) (MLS estimations of parameters of the interface noise component).

(4) To estimate the coordinates of the object position according to equation (19) on the digital image from which the noise photons were excluded earlier. Initial values of the coordinates of the object position should be equal to the coordinates of the central local maximum of the AIFP image (AIFP centre). The following process is used:

(a) to calculate the coefficients of splitting λ_{ikt} according to equation (10);

(b) to estimate the coordinates of the object position on the CCD frame according to equation (9);

(c) to obtain a standard deviation estimate of photons hitting from the object, according to equation (11);

(d) to determine the values of weights of the discrete mix of probability distributions according to equation (12);

(e) to compare the actual value and the value obtained in the previous step – if the difference between them is greater than a predetermined value, the actual value is supplied to (a) as the estimate of the previous step, otherwise, it is sent to the algorithm output as the result of its work.

An important step in the automated pipeline is the creation of a catalogue of stationary objects (blobs) in the frame series. All the objects of this catalogue should be excluded in the next stages of processing, but a few objects should be left as reference stars for astrometry. Thus, those measurements that are absent in the catalogue of stationary objects have been used to select moving objects. With this aim, the original method of collecting light (collection light technology) is provided. Candidates for small Solar system bodies (e.g. asteroids) selected by this method should have about the same brightness on different frames and their coordinates should not deviate significantly from their average trajectory. In the case of partial occultation of a star by an asteroid, more often they stand out as two different celestial objects, in which case the position accuracies of the star and asteroid are reduced. In general, detection of an asteroid is provided at the step of blobs, while the images themselves are not involved in processing (in this situation, the blobs are formed according to the object images).

4 RESULTS AND DISCUSSION

The proposed method provides accurate estimation of asteroid coordinates on a set of CCD frames and is the basis of the CoLiTec software, which has been installed at several observatories in the world since 2009 March 1 (see also Fig. 1).

In 2010 April, CoLiTec was installed at Andrushivka Astronomical Observatory (A50), Ukraine, and already in 2010 May two asteroids were discovered (it was the first discovery of asteroids in the automatic mode at the observatories of the CIS countries). On 2010 November 27, this software was installed at International Scientific Optical Network New Mexico (ISON-NM) (H15, New Mexico, USA) and on 2010 December 10 the comet C/2010 X1 was discovered by L. Elenin. In 2012 July, the CoLiTec software was installed at International Scientific Optical Network Kislovodsk (ISON-Kislovodsk) (D00, Russia) and on 2012 September 21 the comet C/2012 S1(ISON) was discovered by V. Nevsky and A. Novichonok, amateur astronomers. Digital images of the discoveries of these comets are given in Fig. 2(a) and (b), respectively. As we mentioned in the Introduction, in total four comets and more than

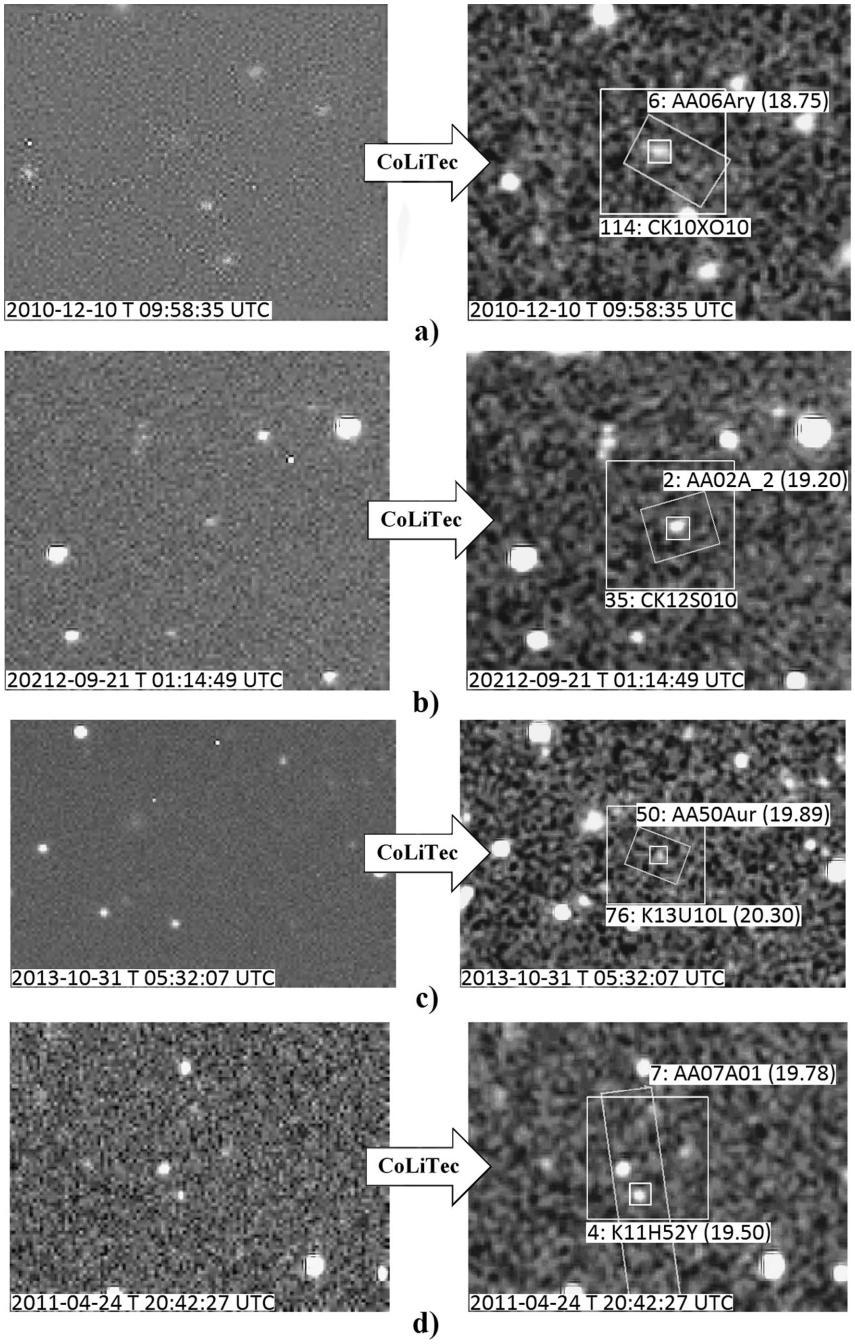

Figure 2. The best-known small Solar system bodies detected and discovered with the CoLiTec software based on the subpixel Gaussian model: (a) the long-period Comet C/2010 X1 (Elenin), having an image size of 5 pixels, has been shifted by 7 pixels on a set of four CCD frames; (b) Comet C/2012 S1 (ISON), having an image size of 5 pixels, has been shifted by 3 pixels on a set of four CCD frames; (c) Centaur object 2013 UL10, having an image size of 5–6 pixels, has been shifted by 2 pixels; (d) the K11H52Y asteroid, having an image size of 5 pixels, has been shifted by 45 pixels on a set of three CCD frames (it is described as unusual in the MPC Circular; see http://www.minorplanetcenter.net/mpec/K11/K11J02.html).

1500 asteroids have been discovered with this software since 2010 (two examples of asteroid discoveries are demonstrated in Fig. 2(c) and (d); the latter object, discovered at Andrushivka Astronomical Observatory on 2011 April 24, is marked as an unusual K11H52Y asteroid in the Minor Planet Center (MPC) Circular).

Since this method was already in operatation during the asteroid observational surveys, we are able to provide a comparative analysis of the statistical parameters of accuracy estimations from this method and other results of the 30 observatories rated the most productive in terms of the number of asteroid observations in 2011–2013 (Tables 1–3). Those observatories that work with only one object in the centre of the CCD frame during a calm and at a suitable phase of the Moon are excluded from our analysis. Those observatories where the CoLiTec software based on this method

Table 1. Accuracy parameters for the 30 observatories that were the most productive in the number of asteroid measurements in 2011, according to the MPC data.

(1) *N*	(2) Observatory code	(3) Measurements, objects	(4) Discoveries	(5) *D* (m)	(6) S_{pix}	(7) RA ($\bar{\Delta}_\alpha/\sigma_\alpha$)	(8) Dec. ($\bar{\Delta}_\delta/\sigma_\delta$)	(9) σ''	(10) σ_{pix}	(11) ARM
1	G96	2106367, 382737	21770	1.50	1.00	−0.01 +/− 0.32	−0.04 +/− 0.28	0.300	0.30	0.041
2	704	1956368, 279129	495	1.00	2.20	0.25 +/− 0.66	0.43 +/− 0.64	0.650	0.29	0.497
3	F51	1557902, 351923	13628	1.80	0.30	0.05 +/− 0.16	0.06 +/− 0.17	0.165	0.55	0.078
4	703	1512387, 259412	2995	0.68	2.60	−0.21 +/− 0.67	0.17 +/− 0.68	0.675	0.25	0.270
5	691	811571, 154495	8356	0.90	1.00	−0.16 +/− 0.33	0.10 +/− 0.30	0.315	0.315	0.189
6	E12	219903, 52808	327	0.50	1.80[1]	−0.04 +/− 0.49	0.32 +/− 0.48	0.485	0.26	0.322
7	645	208656, 45961	7	2.50	0.39					
8	D29	185303, 43414	318	1.04	1.70					
9	C51	162900, 15412	23	0.40	2.75	0.06 +/− 0.57	−0.03 +/− 0.65	0.610	0.22	0.067
10	**H15**	**154970, 37495**	**768**	**0.45**	**2.00**	**−0.03 +/− 0.49**	**0.06 +/− 0.54**	**0.515**	**0.25**	**0.067**
11	106	75340, 18093	73	0.60	2.00	0.04 +/− 0.36	−0.11 +/− 0.35	0.355	0.17	0.117
12	291	70355, 19028	646	1.80	0.60	−0.13 +/− 0.36	0.15 +/− 0.27	0.315	0.52	0.191
13	J75	48469, 13209	561	0.45	1.47	−0.04 +/− 0.42	−0.14 +/− 0.40	0.410	0.28	0.146
14	644	34164, 6255	954	1.20	1.00					
15	**A50**	**33386, 9755**	**72**	**0.60**	**2.06**	**−0.03 +/− 0.51**	**0.05 +/− 0.51**	**0.510**	**0.24**	**0.058**
16	926	28578, 8460	171	0.81, 0.41	0.87	0.15 +/− 0.38	0.27 +/− 0.39	0.385	0.44	0.309
17	461	28038, 6281	782	0.60, 1.02	1.10	−0.03 +/− 0.27	0.14 +/− 0.27	0.270	0.24	0.143
18	A14	24354, 6448	115	0.50		0.08 +/− 0.41	−0.06 +/− 0.36	0.385		0.100
19	J04	23322, 6460	188	1.00	0.62[2]	0.16 +/− 0.29	0.24 +/− 0.30	0.295	0.47	0.288
20	A77	21677, 5423	318	0.50		0.027 +/− 0.63	0.22 +/− 0.50	0.565		0.348

Notes. [1]Mahabal et al. (2011), [2]Li et al. (1999), [3]Benkhaldoun et al. (2012).
Highlighted columns are CoLiTec users.

Table 2. Accuracy parameters for the 30 observatories that were the most productive in the number of asteroid measurements in 2012, according to the MPC data.

(1) *N*	(2) Observatory code	(3) Measurements, objects	(4) Discoveries	(5) *D* (m)	(6) S_{pix}	(7) RA ($\bar{\Delta}_\alpha/\sigma_\alpha$)	(8) Dec. ($\bar{\Delta}_\delta/\sigma_\delta$)	(9) σ''	(10) σ_{pix}	(11) ARM
1	G96	2080033, 384204	17676	1.50	1.00	0.20 +/− 0.33	0.20 +/− 0.28	0.305	0.305	0.028
2	F51	1948353, 467091	13785	1.80	0.30	0.07 +/− 0.15	0.04 +/− 0.17	0.16	0.53	0.081
3	703	1723293, 282864	2278	0.68	2.60	−0.22 +/− 0.65	0.07 +/− 0.62	0.635	0.24	0.231
4	704	1681504, 262209	224	1.00	2.20	0.26 +/− 0.67	0.43 +/− 0.64	0.655	0.29	0.502
5	691	896972, 163714	7600	0.90	1.00	−0.16 +/− 0.32	0.10 +/− 0.29	0.305	0.27	0.189
6	E12	259295, 62621	430	0.50	1.80[1]	−0.01 +/− 0.51	0.29 +/− 0.50	0.505	0.28	0.290
7	J43	102641, 22682	531	0.50[2]	1.20[2]	0.19 +/− 0.48	0.05 +/− 0.40	0.44	0.36	0.196
8	926	100161, 29986	454	0.81, 0.41	0.87	0.02 +/− 0.37	0.05 +/− 0.35	0.36	0.41	0.54
9	**H15**	**97878, 24170**	**338**	**0.45**	**2.00**	**−0.06 +/− 0.50**	**−0.01 +/− 0.53**	**0.515**	**0.25**	**0.061**
10	106	72192, 17451	120	0.60	2.00	0.04 +/− 0.36	−0.12 +/− 0.34	0.35	0.17	0.126
11	A14	57243, 16239	159	0.50		0.06 +/− 0.37	−0.02 +/− 0.32	0.345		0.063
12	J04	43209, 10708	513	1.00	0.62[3]	0.21 +/− 0.28	0.20 +/− 0.27	0.275	0.44	0.29
13	**D00**	**31494, 7403**	**61**	**0.40**	**2.06**	**0,00 +/− 0,57**	**−0,06 +/− 0,41**	**0,49**	**0,23**	**0.06**
14	291	24272, 6224	28	1.80	0.60	0.07 +/− 0.33	0.13 +/− 0.28	0.305	0.50	0.148
15	461	23847, 5615	170	0.60, 1.02	1.10	0.00 +/− 0.27	0.15 +/− 0.27	0.27	0.24	0.15
16	644	22714, 4486	332	1.20[4]	1.00[4]					
17	H21	22672, 3870	181	0.61, 0.81, 0.76	0.80[2]	0.03 +/− 0.34	0.01 +/− 0.36	0.35	0.43	0.032
18	I41	21245, 2392	1790	1.20[5]	1.01[5]	0.11 +/− 0.23	−0.03 +/− 0.23	0.23	0.22	0.114
19	A24	18940, 2412	0	0.36	1.40	0.14 +/− 0.37	0.24 +/− 0.33	0.35	0.25	0.278
22	**A50**	**11559, 3725**	**13**	**0.60**	**2.07**	**0.25 +/− 0.50**	**−0.04 +/− 0.46**	**0.48**	**0.23**	**0.253**

Notes. [1]Mahabal et al. (2011), [2]Benkhaldoun et al. (2012), [3]Abreu & Kuusela (2011), [4]http://neat.jpl.nasa.gov/neatoschincam.htm, [5]Waszczak et al. (2013).
Highlighted columns are CoLiTec users.

Table 3. Accuracy parameters for the 30 observatories that were the most productive in the number of asteroid measurements in 2013, according to the MPC data.

(1) N	(2) Observatory code	(3) Measurements, objects	(4) Discoveries	(5) D (m)	(6) $S_{\rm pix}$	(7) RA ($\bar{\Delta}_\alpha/\sigma_\alpha$)	(8) Dec. ($\bar{\Delta}_\delta/\sigma_\delta$)	(9) σ''	(10) $\sigma_{\rm pix}$	(11) ARM
1	F51	2279609, 506894	14168	1.80	0.30	0.13 +/− 0.07	0.06 +/− 0.14	0.135	0.45	0.092
2	G96	1950642, 343808	11908	1.50	1.00	0.04 +/− 0.32	0.05 +/− 0.28	0.300	0.30	0.064
3	703	1844330, 289086	1494	0.68	2.60	−0.14 +/− 0.66	0.22 +/− 0.64	0.650	0.25	0.260
4	691	742001, 139225	5594	0.90	1.10	−0.16 +/− 0.31	0.12 +/− 0.30	0.315	0.28	0.200
5	D29	551094, 136964	262	1.04	1.70	0.03 +/− 0.53	−0.04 +/− 0.49	0.510	0.30	0.050
6	I41	440712, 52579	2270	1.20[1]	1.01[1]	0.06 +/− 0.18	0.02 +/− 0.17	0.175	0.17	0.063
7	E12	229747, 48026	204	0.50	1.80[2]	−0.02 +/− 0.50	0.28 +/− 0.46	0.480	0.26	0.280
8	926	179570, 53662	750	0.81, 0.41	0.87	0.15 +/− 0.39	0.10 +/− 0.36	0.375	0.43	0.180
9	J43	151983, 27006	1006	0.50[3]	1.20[3]	0.11 +/− 0.31	−0.03 +/− 0.29	0.300	0.25	0.114
10	W84	110213, 8518	4160	40[3, 4]	0.27[4]	0.13 +/− 0.13	0.14 +/− 0.13	0.130	0.48	0.191
11	**H15**	**107989, 25282**	**156**	**0.40**	**2.00**	**0.09 +/− 0.62**	**0.02 +/− 0.60**	**0.610**	**0.305**	**0.092**
12	704	81054, 17833	4	1.00	2.20	0.29 +/− 0.64	0.38 +/− 0.63	0.635	0.28	0.478
13	J04	58307, 14670	576	1.00	0.62[5]	0.25 +/− 0.30	0.23 +/− 0.28	0.290	0.46	0.340
14	**D00**	**44658, 10850**	**34**	**0.40**	**2.06**	**0.01 +/− 0.72**	**−0.12 +/− 0.54**	**0.630**	**0.305**	**0.120**
15	G32	36416, 4654	654	0.40	1.13	0.03 +/− 0.35	0.05 +/− 0.32	0.335	0.29	0.058
16	106	18601, 4502	67	0.60	2.00	0.04 +/− 0.39	−0.05 +/− 0.37	0.370	0.19	0.064
17	H21	16924, 2994	60	0.61, 0.81, 0.76	0.80[6]	0.04 +/− 0.33	−0.04 +/− 0.31	0.320	0.4	0.002
18	461	15688, 3787	110	0.60, 1.02	1.10	−0.02 +/− 0.24	0.17 +/− 0.27	0.255	0.23	0.171
19	644	15221, 3317	63	1.20[7]	1.00[7]					
20	291	15197, 4002	1	1.80	0.60	0.02 +/− 0.35	0.14 +/− 0.32	0.335	0.55	0.141

Notes. [1]Waszczak et al. (2013), [2]Mahabal et al. (2011), [3]Benkhaldoun et al. (2012), [4]Honscheid & DePoy (2008), [5]Abreu & Kuusela (2011), [6]Li et al. (1999), [7]http://neat.jpl.nasa.gov/neatoschincam.htm.
Highlighted columns are CoLiTec users.

was installed work both during gusts and when it is calm. Moreover, the method is adaptive in such a way that there is no problem in automatic processing of object images on the CCD frames both in the centre and at its edges, as well as providing measurements of many objects on a single frame.

Therefore, during years 2011–2013, observatories such as the ISON-NM Observatory (H15: Elenin, Savanevych & Bryukhovetskiy 2012, 2013b), Andrushivka Astronomical Observatory (A50: Ivashchenko & Kyrylenko 2011; Ivashchenko, Kyrylenko & Gerashchenko 2012, 2013) and ISON-Kislovodsk Observatory (D00) acted as users of the CoLiTec software (Elenin et al. 2014). In the ranking of the most productive observatories worldwide in 2012, based on the number of discoveries of small Solar system bodies, the users of the CoLiTec software had the third, 13th and 22nd places, respectively. In the final report of 2011–2012, the ISON-NM Observatory (H15) holds the seventh place both by number of measurements and by priority of discoveries.

In Tables 1–3, the total numbers of measurements and objects (column 3) as well as asteroid discoveries (column 4) are given, according to the MPC circulars of 2011, 2012 and 2013, respectively (Minor Planet Center 2013a). The statistical parameters of these measurements are taken from the MPC site (http://www.minorplanetcenter.net/iau/special/residuals2.txt). The following parameters are also indicated in the tables for each observatory: diameter D of the primary mirror of the telescope in metres (column 5); scale $S_{\rm pix}$ of the pixel image in arcsec (column 6); average residuals $\bar{\Delta}_\alpha$ and $\bar{\Delta}_\delta$ of object positions in right ascension α and declination δ at a predetermined time (column 7); standard deviation estimations σ_α and σ_δ of object positions in right ascension α and declination δ at a predetermined time (column 8); standard deviation estimations σ'' of object position (equation 20) in arcsec (column 9); standard deviation estimations $\sigma_{\rm pix}$ of object position (equation 21) in pixels (column 10); module of average residuals of object position measurements (ARM, equation 22) (column 11). To calculate some of the aforementioned parameters, we applied the following formulae:

$$\sigma'' = 0,5(\sigma_\alpha + \sigma_\delta), \tag{20}$$

$$\sigma_{\rm pix} = \frac{\sigma''}{S_{\rm pix}}, \tag{21}$$

$$\mathrm{ARM} = \sqrt{(\bar{\Delta}_\alpha)^2 + (\bar{\Delta}_\delta)^2}. \tag{22}$$

The data analysis related to the accuracy parameters of object position for the most productive observatories as regards the number of asteroid measurements in 2011–2013 is illustrated in Fig. 3.

The observatory partners of the CoLiTec programme hold leading positions in their class of telescopes, related to the parameter of the module of average residuals of measurements (Fig. 3a). In 2011 and 2012, this parameter was equal to 0.06 arcsec for the H15 (Elenin et al. 2012) and A50 observatories. At the same time, these observatories were not in the list of best observatories as related to the parameters of standard deviation estimations of object position (in arcsec) (see Fig. 3c and d). In 2011, the values of the standard deviation estimations σ'' of object position for the observatories mentioned were equal to 0.515 arcsec (H15) and 0.51 arcsec (A50). In 2012, these values were equal to 0.515 arcsec (H15), 0.49 arcsec (D00) and 0.48 arcsec (A50). The reason for such a deterioration of the results, in addition to the size of aperture of the telescope, is the pixel scale of the CCD matrix used. To take this factor into account, the observatory partners of the CoLiTec programme decided to consider the parameter of standard deviation estimations $\sigma_{\rm pix}$ of the object position in pixels for accurate estimation of asteroid coordinates on the CCD frame as a principal parameter during observations.

The parameter of standard deviation estimations $\sigma_{\rm pix}$ of the object position in pixels on the CCD frame (Fig. 3b; column 10 in Tables 1–3) is used to characterize the efficiency of the mathematical method applied for coordinate measurements. In other words, it allows the observer to be disengaged from the parameters of the CCD matrix

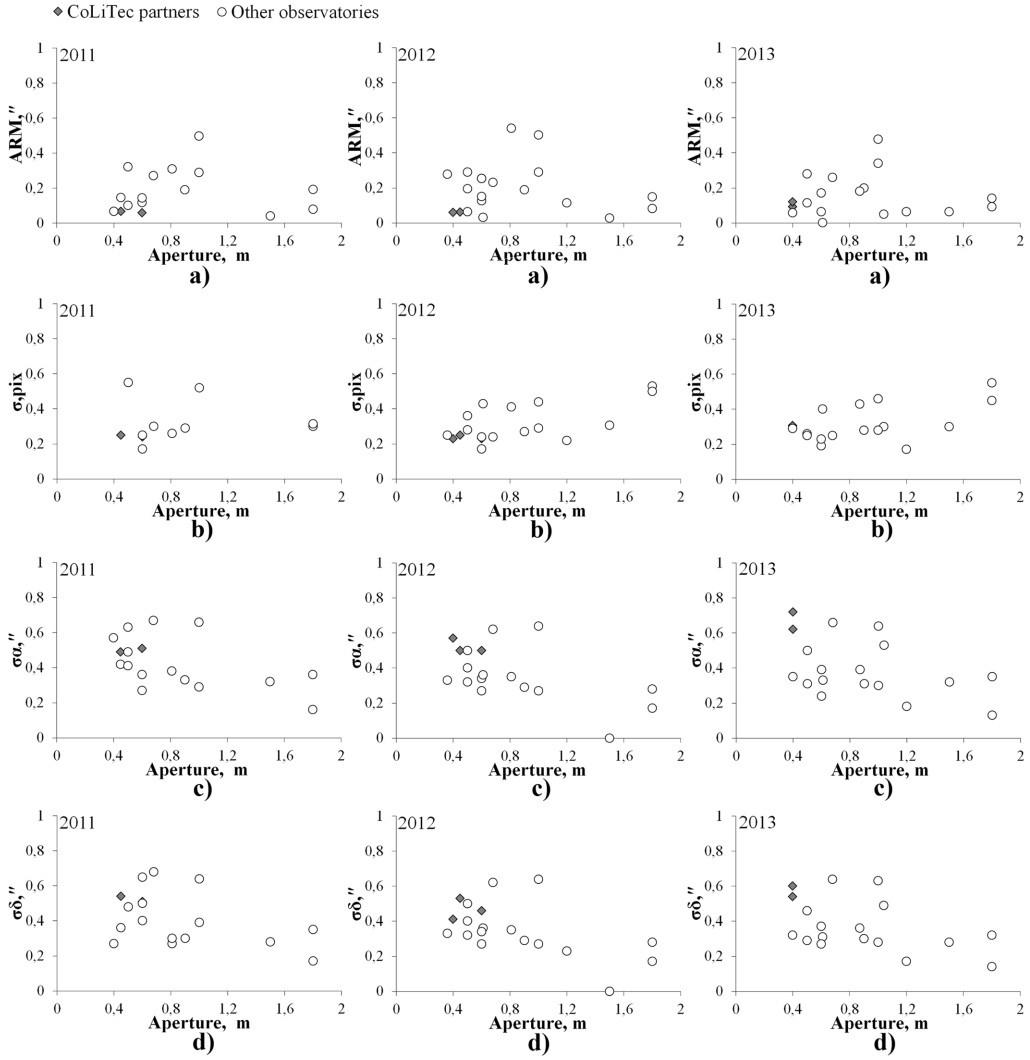

Figure 3. Comparative analysis of the accuracy parameters for object position for the most productive observatories using the number of asteroids measurement in 2011 (left), 2012 (middle) and 2013 (right): (a) module of average residuals of object position measurements; (b) standard deviation estimations $\sigma_{\rm pix}$ of object position in pixels; (c) standard deviation estimations of object position in right ascension, σ_α, in arcsec; (d) standard deviation estimations of object position in declination, σ_δ, in arcsec.

and other devices used. According to this parameter, the observatory partners of the CoLiTec programme have one of the best results among observatories in their class of telescopes (small aperture). In 2011 (2012), this parameter was equal to 0.25 (0.25) pixel and 0.24 (0.23) pixel for observatories H15 and A50, respectively, and was equal to 0.23 pixel for observatory D00 in 2012. In 2013, the accuracy of measurements of the observatories (CoLiTec partners) fell by approximately 20 per cent for all the parameters mentioned, due to an error in the software that was immediately fixed and completely corrected. As a result, the observatory partners of the CoLiTec programme returned to their previous positions as regards indexes of measurement accuracy (see the current MPC site for details). It is important to emphasize that the standard deviation $\sigma_{\rm pix}$ of object position (Fig. 3b) is an artificial parameter. It is not a strong objective, because factors such as the exposure time, telescope optical scheme, height above sea level and many others are not taken into account in it. For example, according to this parameter, the Pan-STARRS 1 observatory (F51) had lost positions, although it had the best astrometry accuracy among all asteroid surveys. We suggest that an implementation of our method, which is free from possible loss of measurement information contained on the CCD frames, when used at this observatory could most likely yield the best results possible.

We also compared the CoLiTec software with the Astrometrica software, which is widely accepted among amateurs.

Both software packages realize the following functions: frame calibration; support for astrometric and photometric catalogues of stars in local and online modes; recording of coordinate information (WCS) in the FITS-frame title; interactive mode for object position measurements; magnifier tool; an automated search of moving objects; a mode for visual inspection of moving objects detected; provision for output of astrometric measurements in the MPC format; transferral of data mode from the interface to the MPC; display of known and discovered objects on the CCD frame. However, CoLiTec does not realize functions such as 'Track & Stack' for adding the frame or identification of detected moving objects with a local data base Minor Planet Center Orbit (MPCORB).

At the same time, unlike Astrometrica, CoLiTec does the following: realizes functions such as astrometric reduction of CCD frames with large fields of view (2° or more); separates application

of reference catalogues for astrometric and photometric reduction; provides an automated search of moving faint objects (SNR 2.5); has automatic data processing; saves results on the processing frames (real detected objects, objects rejected by the operator, etc.); identifies detected moving objects with the online data base MPCORB (MPC); identifies stationary objects with a data base of variable stars (VSX) and galaxies (HyperLeda); has a software modular design (the ability to connect individual modules). The CoLiTec software gives more accurate measurements of faint celestial objects, as well as containing a more reliable method for identifying frames with a reference star catalogue, allowing us to improve (sometimes significantly) the accuracy of an object position.

Along with an analysis of indexes of measurement accuracy (see the current MPC site), we conducted a comparative analysis of the accuracy of both software packages (CoLiTec versus Astrometrica) after processing the same frame. We selected 19 series for each of the four frames. A preliminary analysis included 36 series. However, the rest of the series had no reliable identification with the star catalogue used. Also, we excluded frames with significant disruptions in the daily maintenance and frames taken at very high wind. All frames were obtained at the observatory ISON-NM (H15) with the help of a 40-cm telescope Santel-400AN and CCD-matrix FLI ML09000-65 (3056 × 3056 pixels, a pixel size of 12 μm) during the period 2014 March 4–March 30. The exposure time was 150 s.

We used only object positions with measurements included in the MPCAT-OBS archive (MPCAT-OBS) http://www.minorplanetcenter.net/iau/ECS/MPCAT-OBS/MPCAT-OBS.html. The measurements, however, were reprocessed with the CoLiTec software. To set reference values of object positions at the time of measurement formation, we used the HORIZONS service (HORIZONS) http://ssd.jpl.nasa.gov/?horizons. In total, we used 2002 measurements (measurements with CoLiTec were performed on 253 more occasions). Astrometrica in several cases issued a warning regarding impossibility to guarantee a reliable measurement of object position (Centroid $= -1$). This is often associated with an attempt to measure the position of star trails or faint objects involved with a brighter star. More than half of these have SNR not exceeding 3.5. The results of the comparative analysis are shown in Table 4. One can see that measurements with Astrometrica at low SNR have a root-mean-square error (MSE) 30–50 per cent larger than that of CoLiTec (see also Figs 4 and 5). Mean deviations in measurements with CoLiTec and Astrometrica are the same in general and so these data are not shown. A more detailed comparative analysis is given in another of our articles (Savanevych et al. 2015).

Table 4. Comparative analysis of the CoLiTec and Astrometrica software as regards measurements of object positions for numbered asteroids.

(1) Deviation	(2) Astrometrica	(3) CoLiTec
Average deviation of RA (arcsec)	0,11	0,11
Average deviation of DE (arcsec)	– 0,04	– 0,03
RMS deviation of RA (arcsec)	0,77	0,50
RMS deviation of RA (arcsec)	0,67	0,39

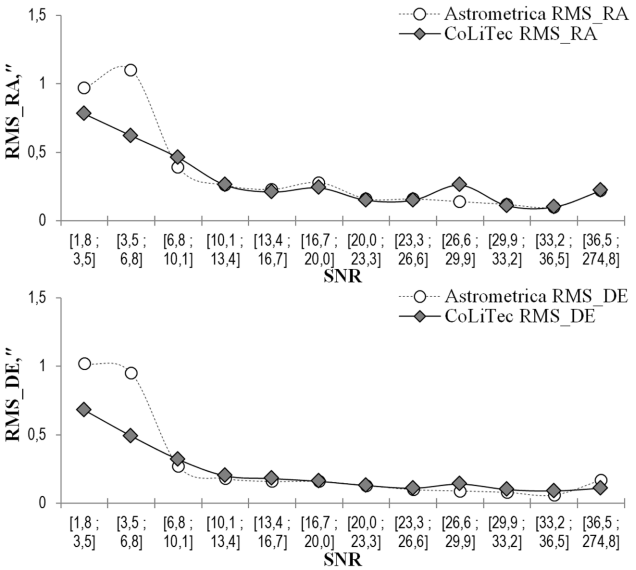

Figure 4. Distribution of deviations of the equatorial coordinates of objects by SNR range (Astrometrica versus CoLiTec).

5 CONCLUSIONS

A new iteration method for asteroid coordinate estimation on digital images has been developed. The method operates by continuous parameters (asteroid coordinates) in a discrete observation space (the set of pixels potential of the CCD matrix).

High indices of the CoLiTec programme during 2011–2012 as concerns with the accuracy of measurements have been obtained due to the use of the subpixel Gaussian model. This model of the object image takes into account the prior form of the object image and consequently it is adapted more flexible to any form of real image. In other words, even if the real coordinate distribution of photons hitting pixels on the CCD frame is not known, the form of this distribution is known a priori and its parameters can be estimated according to the real object image. Currently, many other methods mentioned in the Introduction consider by default that the density of hit photons inside the pixel is uniform.

The advantages of a subpixel Gaussian model become more obvious for fainter celestial objects. Moreover, the method developed has a high measurement accuracy as well as a low calculating complexity, because a maximum-likelihood procedure is implemented to obtain the best fit, instead of the least-squares method and Levenberg–Marquardt algorithm for minimization of the quadratic form.

The efficiency of the proposed method, including its advantages for accurately estimating asteroid coordinates, was confirmed during observations as the part of the CoLiTec programme for automatic discoveries of asteroids and comets on a set of CCD frames. Efficiency is a crucial factor in the discovery of near-Earth asteroids (NEA) and potentially hazardous asteroids. Current asteroid surveys yield many images per night. It is no longer possible for the observer to view these images quickly in the blinking mode. This causes serious difficulty for large-aperture wide-field telescopes, which capture up to several tens of asteroids in one image. The CoLiTec software solves the problem of frame-processing for asteroid surveys in a real-time mode. We also compared our software with Astrometrica, which is widely used for detecting new objects. The limits of measurements of the CoLiTec software are wider than those of Astrometrica but, most valuably, this expansion comes in an area of extremely small SNR, allowing us to search for fainter Solar system small bodies (measurements with Astrometrica at a low SNR have an RMS 30–50 per cent larger than that of CoLiTec). For the area with SNR > 7, the results of CoLiTec and Astrometrica

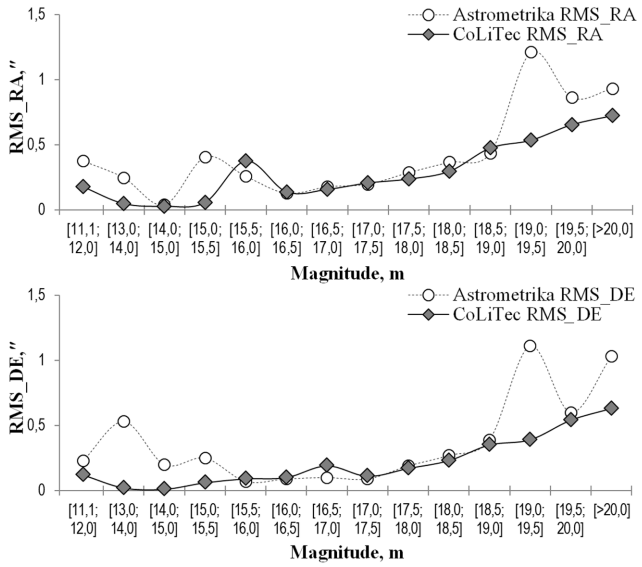

Figure 5. Distribution of deviations of the equatorial coordinates of objects by magnitude range (Astrometrika versus CoLiTec).

are approximately identical. However, the area of extremely small SNR is more promising for the discovery of new celestial objects.

The automatically detected small Solar system bodies are subject to follow-up visual confirmation. The CoLiTec software is in use for the automated detection of asteroids at Andrushivka Astronomical Observatory, Ukraine (since 2010), the Russian remote observatory ISON-NM (Mayhill, New Mexico, USA) since 2010, the observatory ISON-Kislovodsk since 2012 and the ISON-Ussuriysk observatory since 2013 (see Tables 1–3). As a result, four comets (C/2010 X1 (Elenin), Elenin et al. 2010; P/2011 NO1 (Elenin), Elenin et al. 2011, Elenin, Savanevych & Bryukhovetskiy 2013a; C/2012 S1 (ISON), Nevski 2012; and P/2013 V3 (Nevski), Nevski 2013) as well as more than 1500 small Solar system bodies (including five NEOs, 21 Trojans of Jupiter and one Centaur object) have been discovered.

In 2014, the CoLiTec software was recommended to all members of the *Gaia* Follow-Up Network for ground-based observation of peculiar Solar System Objects (*Gaia*-FUN-SSO) for analysing observations as a tool to detect faint moving objects in frames. Information about CoLiTec, with a link to the website, has been posted on the *Gaia*-FUN-SSO[1] Wiki.

ACKNOWLEDGEMENTS

The authors thank Dr F. Velichko for his useful comments. We are grateful to the reviewer for helpful remarks that improved this work. We express our gratitude to Mr W. Thuillot, coordinator of the *Gaia*-FUN-SSO network, for the approval of CoLiTec as software well-adapted to the *Gaia*-FUN-SSO conditions of observation. We also thank Dr Ya. Yatskiv for his support of this work in frames of the Target Program of Space Science Research of the National Academy of Science of Ukraine (2012–2016) and the Ukrainian Virtual Observatory (http://www.ukr-vo.org). The CoLiTec programme is available through http://colitec.neoastrosoft.com/en (one can access the download package http://www.neoastrosoft.com/download_en and some instructions at http://www.neoastrosoft.com/documentation_en).

[1] https://www.imcce.fr/gaia-fun-sso/

REFERENCES

Abreu D., Kuusela J., 2013, Upgraded camera for ESA optical space surveillance system. In 35 European Space Surveillance Conference 7–9 June 2011, INTA HQ, Madrid, Spain, available at: http://www.infoespacial.com/wp-content/uploads/11c01-abstractbook-v8.pdf

Bauer T., 2009, Improving the Accuracy of Position Detection of Point Light Sources on Digital Images. In Proceedings of the IADIS Multiconference, Computer Graphics, Visualization, Computer Vision and Image Processing, Algarve, Portugal, June 20–22, 2009, p. 3

Benkhaldoun Z., Rinner C., Ory M., Daassou A., Colas F., 2012, The Morocco Oukaimeden Sky Survey, the MOSS Telescope. LPI Contributions, 1667, 6182

Burden R. L., Faires J. D., 2010, Numerical Analysis 9th ed. Brooc/Cole, 877

Dell'Oro A., Cellino A., 2012, Planet. Space Sci., 73, 10

Elenin L. et al., 2010, Central Bureau Electronic Telegrams, 2384, 1

Elenin L. et al., 2011, Central Bureau Electronic Telegrams, 2768, 1

Elenin L., Savanevych V., Bryukhovetskiy A., 2012, Minor Planet Circulars, 81836, 6

Elenin L., Savanevych V., Bryukhovetskiy A., 2013a, Minor Planet Circulars, 82408, 43

Elenin L., Savanevych V., Bryukhovetskiy A., 2013b, Minor Planet Circulars, 82692, 1

Elenin L., Molotov I., Savanevych V., Krugly Y., Bruhovetskiy A., Ivaschenko Y., 2014, in Muinonen K. et al., eds, ASPIN–ISON asteroid program: History, current state, and future prospects. In Asteroids, Comets, Meteors 2014, Conf. Proc., 30 June–4 July 2014, Helsinki, Finland

Faraji H., MacLean W. J., 2006, Image Processing, IEEE Trans., 15, 2676

Gary B. L., Healy D., 2006, Bull. Minor Planets Section Assoc. Lunar Planet. Observers, 33, 16

Gural P. S., Larsen J. A., Gleason A. E., 2005, AJ, 30, 1951

Harris W. E., 1990, PASP, 102, 949

Honscheid K., DePoy D. L., 2008, The Dark Energy Camera (DECam) A new instrument for the Dark Energy Survey. In Nuclear Science Symposium Conference Record, NSS'08, IEEE, 3357

Ivashchenko Yu., Kyrylenko D., 2011, Minor Planet Circulars, 77269, 7

Ivashchenko Yu., Kyrylenko D., Gerashchenko O., 2012, Minor Planet Circulars, 81732, 6

Ivashchenko Yu., Kyrylenko D., Gerashchenko O., 2013, Minor Planet Circulars, 82554, 3

Izmailov I. S. et al., 2010, Astron. Lett., 36, 349

Jogesh Babu G., Mahabal A. A., Djorgovski S. G., Williams R., 2008, Statistical Methodology, 5, 299

Lafreniere D., Marois C., 2007, ApJ, 660, 770

Li W. D. et al., 1999, The Lick Observatory Supernova Search, preprint (arXiv:astro-ph/9912336v1)

Lo Y., Mendell N. R., Rubin D. B., 2001, Biometrika, 88, 767

Mahabal A. A. et al., 2011, Bull. Astron. Soc., 39, 387

Miura N., Itagaki K., Baba N., 2005, AJ, 130, 1278

Nevski V., 2012, Minor Planet Circulars, 80063, 14

Nevski V., 2013, Minor Planet Electronic Circ., 45, available at: http://www.minorplanetcenter.net/mpec/K13/K13V45.html

O'Sullivan C. M. et al., 1999, The mesospheric sodium layer at Calar Alto, Spain. Astronomy with adaptive optics-Present results and future programs, 56, 333

Savanevych V. E., 1999, Radio Electronics and Informatics, 1, 4

Savanevych V. E., 2006, Models and the data processing techniques for detection and estimation of parameters of the trajectories of a compact group of space small objects. D.Sci. thesis, Kharkiv National University for Radio Electronics, Kharkiv, 446 pp. (in Russian)

Savanevych V. E., Briukhovetskyi O. B., Kozhuhov A. M., Dikov E. M., 2010, Radiotekhnika: All-Ukrainian Interagency Scientific and Engineering Journal, 162, 78 (in Russian)

Savanevych V. E., Kozhukhov O. M., Briukhovetskyi O. B., Vlasenko V. P., Dikov E. M., Ivashchenko Yu. M., Elenin L., 2011, Program of Automatic Asteroid Search and Detection on Series of CCD-Images. In Lunar and Planetary Inst. Technical Report, 42, 1140

Savanevych V. E., Briukhovetskyi O. B., Kozhuhov A. M., Dikov E. M., Vlasenko V. P., 2012, Kosmichna Nauka i Tekhnologiya, 18, 39

Savanevych V., Bryukhovetskiy A., Sokovikova N., Bezkrovniy M., Khlamov S., Elenin L., Movsesian I., Dihtyar M., 2014, in Muinonen K. et al., eds, Automated software for CCD-image processing and detection of small Solar system bodies. Asteroids, Comets, Meteors 2014, Conf. Proc., 30 June–4 July 2014, Helsinki, Finland

Savanevych V. E. et al., 2015, Kinematics and Physics of Celestial Bodies, 31, 64

Vavilova I. B. et al., 2011, Kosmichna Nauka i Tekhnologiya, 17, 74

Vavilova I. B. et al., 2012, Kinematics and Physics of Celestial Bodies, 28, 85

Vavilova I. B., Pakuliak L. K., Protsyuk Yu. I., Shlyapnikov A. A., Savanevich V. E., Kondrashova N. N., Yatsenko A. I., Andruk V. N., 2012, Baltic Astron., 21, 356

Veres P., Jedicke R., 2012, PASP, 124, 1197

Waszczak A. et al., 2013, MNRAS, 433, 3115

Yanagisawa T., Nakajima A., Kadota Kenichi, Kurosaki H., Nakamura T., Yoshida F., Dermawan B., Sato Y., 2005, PASJ, 57, 399

Zacharias N., 2010, AJ, 139, 2208

This paper has been typeset from a TEX/LATEX file prepared by the author.